32nd EPS Conference on Plasma Phys. Tarragona, 27 June - 1 July 2005 ECA Vol.**29C**, P-1.088 (2005)

Spatial Resolution of Poloidal Correlation Reflectometry

Popov A Yu, Gusakov E Z

Ioffe Institute, St-Petersburg, Russia

1.Introduction

Poloidal correlation reflectometry (PCR) utilizing microwave plasma probing by several poloidaly separated antennae is used nowadays for plasma rotation diagnostics and turbulence analysis [1]. The poloidal rotation velocity (PRV) $V(r)$ is determined in this technique from the temporal shift τ_{cor} of the maximum of the cross correlation function of scattered signals in two poloidaly separated channels $V(r_c) = \delta_\vartheta a/(\tau_{cor} r_c)$ (see Fig1 for the diagnostic scheme and notations used). The localization of measurements and their interpretation is usually based in PCR on the assumption that the microwave scattering off long scale fluctuations dominating in the turbulence spectra occurs in the cut-off layer. This assumption being correct in respect to backscattering, however fails in the case of small angle scattering or forward scattering, which is possible all over the probing wave trajectory. In spite of the fact the forward scattering is enhanced in the vicinity of cut off [2], this localization is not sufficient to guarantee the suppression of the volume contribution to the PCR signal for all density profiles. In the present paper the localization of PCR is treated analytically in 3D WKB approach for arbitrary density and turbulence profiles in cylindrical geometry.

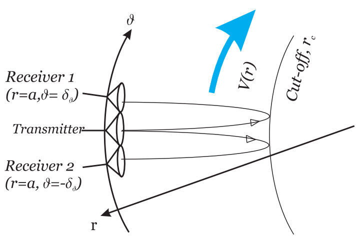

Figure 1 Poloidal correlation reflectometry experimental scheme

2.General approach

The analysis is performed in the cylindrical geometry taking into account the curvature effects. The 1D background plasma density $n_0(r)$ distribution is assumed. The density fluctuations $\delta n(\vec{r},t) = n(\vec{r},t) - n_0(r)$, characterized by the correlation function

$$< \delta n(\vec{r},t)\delta n(\vec{r}',t') >= \delta n^2(R) \cdot \exp\left[-\frac{(r-r')^2}{l_{cr}^2} - \frac{((\vartheta-\vartheta')a - V(R)\tau)^2}{l_{c\vartheta}^2} \right],$$

where $\vec{r} = (r,\vartheta,z)$, $R = r + r'/2$, $\tau = t - t'$, are supposed small, satisfying the Born approximation, whereas the turbulence radial correlation length satisfies condition $l_{cr} > \left(c^2(a-r_c)/\omega^2\right)^{1/3}$, allowing to neglect backscattering far from the cut off. Under above assumptions the incident O mode wave field in plasma can be represented as a superposition of WKB modes propagating at different angles. In particular, at the receiving antennae with the accuracy to the first order in density perturbation amplitude one obtains the following expression for the reflected wave:

$$E(\vartheta,z,t) = (2\pi)^{-2} \sum_m \int \tilde{E} \exp\left(i\phi_r(m,k_z,t)\right) dk_z$$

with $\phi_r(m,k_z,t)$ being WKB phase consisting of the unperturbed term $\varphi_0(m,k_z,t)$ given in paraxial approximation by the expression

$$\varphi_0(m,k_z,t)=2\int_a^{r_c}k(r)dr'+m^2d_\vartheta^2(0)/2a^2+k_z^2d_z^2(0)/2+m\vartheta+k_zz-\frac{\pi}{2},$$

where $k(r)=\frac{\omega}{c}\sqrt{1-n(r)/n_c}$, $d_\vartheta^2(r)=2\int_r^{r_c}\frac{a^2}{r'^2}\frac{dr'}{k(r')}$ and $d_z^2(r)=\frac{2c^2}{\omega^2}\int_r^{r_c}k(r')dr'$, $n_c=n_0(r_c)$ and the phase perturbation $\delta\varphi=-\frac{\omega^2}{2c^2}\cdot\left(\int_a^{r_c}\frac{\delta n(r',\theta^-(r'),z^-(r'),t)}{n_c}\frac{dr'}{k(r')}+\int_a^{r_c}\frac{\delta n(r',\theta^+(r'),z^+(r'),t)}{n_c}\frac{dr'}{k(r')}\right)$

calculated along the unperturbed trajectory that comes to the point (ϑ,z) and is given by relations $\theta^\pm=\vartheta-m\left[d_\vartheta^2(0)\pm d_\vartheta^2(r)\right]/2a^2$, $z^\pm=z-k_z\left[d_z^2(0)\pm d_z^2(r)\right]/2$. The upper and lower signs in the above equations correspond to the parts of the ray trajectory after and before the reflection from the cut off surface. Both the probing and the receiving antennae beams are assumed to be Gaussian with equal the poloidal and toroidal width

$$E_0=\sqrt{a/\pi\rho^2}\exp\left(-\left(a^2\vartheta^2+z^2\right)/2\rho^2\right)=\left(\sqrt{2}\pi\right)^{-2}\sqrt{\pi\rho^2/a}\int dmdk_z\exp\left(-\left(m^2/a^2+k_z^2\right)\rho^2/2\right).$$

The expression for the scattering power in the standard reflectometer case can be represented as

$$P_s=P_i\frac{\omega^4l_{cr}}{c^4}\frac{\int_a^{r_c}\frac{\delta n^2[r]}{n_c^2}\frac{dr}{Q^2(r)}}{\sqrt{1+\frac{d_z^4(0)}{4\rho^4}}\sqrt{1+\frac{d_\vartheta^4(0)}{4\rho^4}}\sqrt{1+\frac{2\rho_\vartheta^2}{l_{c\vartheta}^2}}} \tag{1}$$

where P_i is a probing power and the scattering efficiency $1/Q^2(r)$ takes an explicit form

$$\frac{1}{Q^2(r)}=\begin{cases}\frac{1}{k^2(r)},r-r_c\gg l_{cr}\\ \left[\frac{c^2}{\omega^2}\frac{\sqrt{\pi}\tilde{L}_n}{l_{cr}}\exp\left(-\frac{(r-r_c)^2}{2l_{cr}^2}\right)I_0\left(\frac{(r-r_c)^2}{2l_{cr}^2}\right)\right],r-r_c\le l_{cr},\tilde{L}_n=\left(\frac{d\ln n_0}{dr}\right)_{r=r_c}^{-1}\end{cases} \tag{2}$$

It increases as $1/k^2(r)$ in the cut off vicinity, however this singularity is a week one and does not provide the only input to the integral. In the case of linear density profile and homogeneouse turbulence this so called logarithmic singularity results in substantial contribution of the plasma volume to the signal (1). In this case the scattered signal is related to the density perturbation by the following simple expression

$$\delta n(r_c)=n_c\frac{c}{\omega}\sqrt{\frac{P_s}{P_i}}\left(\left(1+\frac{d_\vartheta^4(a)}{4\rho^4}\right)\left(1+\frac{d_z^4(a)}{4\rho^4}\right)\left(1+\frac{2\rho^2}{l_{c\vartheta}^2}\right)\right)^{1/4}\left[\sqrt{\pi}l_{cr}L_n\left[\ln\left(\frac{8L_n}{\pi l_{cr}}\right)+0.71\right]\right]^{-1/2} \tag{3}$$

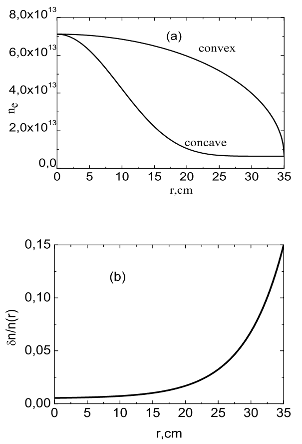

Figure 2 (a) background density profiles (convex and concave); (b) density fluctuation level profile

which can be used for reconstruction of turbulence distribution from the fluctuation reflectometry data. This expression accounts for the contribution of the plasma volume to the signal, however neglects the density profile nonlinearities and turbulence inhomogeneity, which can be very strong at the edge. Relation (3) is used below in figure 3 for reconstruction of the turbulence distribution from measurements performed at variable probing frequency in the case of plasma density and turbulence profiles shown in figure 2. As it is seen in figure 3, the fluctuation reflectometry signal dependence on the cut off position (blue points) does not give an adequate approximation for the turbulence distribution for both profiles. On contrary, expression (3) in the case of concave profile provides a fairly good reconstruction of the turbulence in wide spatial zone. In the case of convex density profile the reconstruction is less perfect, however it can be used as a zero order approximation for the iteration procedure based on (1). The CCF of two signals can be obtained explicitly as

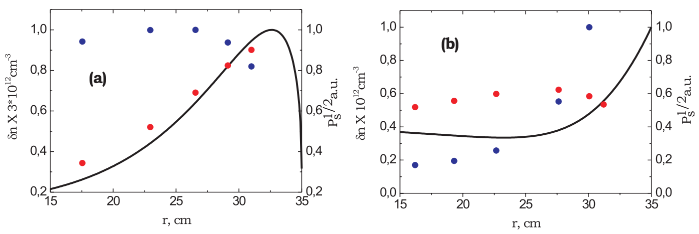

Figure 3 Density fluctuation reconstruction (solid line – original turbulence distribution, blue squares – reflectometry signal, red circles – according to (3)). (a) the case of convex density profile; (b) the case of concave density profile.

$$CCF_{12}(\tau) \simeq \frac{P_i}{\sqrt{P_{s1}P_{s2}}}\frac{\sqrt{\pi}\, l_{cr}}{\sqrt{1+\frac{d_g^4(0)}{4\rho^4}}\sqrt{1+\frac{d_z^4(0)}{4\rho^4}}}\frac{\omega^4}{4c^4}\int_{r_c}^{a}\frac{dr}{Q^2(r)}\frac{\delta n^2(r)}{n_c^2}\left(S_{12}^{++}+S_{12}^{--}+2S_{12}^{-+}\right), \qquad (4)$$

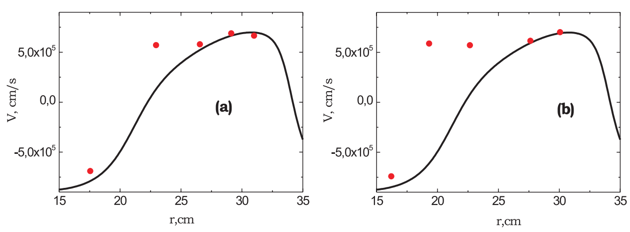

Figure 4 Velocity profile reconstruction (solid line – original profile, circles - profile extracted from PCR; (a) and (b) – correspond to convex and concave density profiles).

where $S_{12}^{++}(r,\tau)+S_{12}^{--}(r,\tau)$ and $2S_{12}^{+-}(r,\tau)$ are the contributions of different (incident-incident, reflected-reflected and incident-reflected) branches of two ray trajectories to the correlation function. These contributions are expressed in terms of elementary functions, in particular

$$S_{12}^{+-}=\frac{\dfrac{l_{c\vartheta}}{\rho_\vartheta}\exp\left\{-\dfrac{2\delta_\vartheta^2\rho_\vartheta^2}{4\rho_\vartheta^4+d_\vartheta^4(a)}\right\}}{\sqrt{1+\dfrac{l_{c\vartheta}^2}{2\rho_\vartheta^2}+\dfrac{d_\vartheta^4(r)}{4\rho_\vartheta^4\left(1+\dfrac{d_\vartheta^4(a)}{4\rho_\vartheta^4}\right)}}}\exp\left(-\frac{\left(r\delta_\vartheta\left[1+\dfrac{d_\vartheta^4(r)d_\vartheta^4(a)}{4\rho_\vartheta^4\left(1+\dfrac{d_\vartheta^4(a)}{4\rho_\vartheta^4}\right)}\right]-V(r)\tau\right)^2}{2\rho_\vartheta^2\left(1+\dfrac{l_{c\vartheta}^2}{2\rho_\vartheta^2}+\dfrac{d_\vartheta^4(r)}{4\rho_\vartheta^4\left(1+\dfrac{d_\vartheta^4(a)}{4\rho_\vartheta^4}\right)}\right)}\right) \qquad (5)$$

As it is pointed out by (4) the scattering efficiency (2) enters the CCF expression, thus providing some cut off localisation to the PRV measurements. However, as in the case of the reflectometry signal, it does not suppress completely the volume contribution, which can, in principle, decrease the locality of the PCR technique. An example of velocity profile reconstruction from the PCR data for density profiles of fig.2 are shown in figure 4. As it is seen there, reconstruction of the velocity profile from PCR data under cut off localisation assumption is more reliable in the case of convex profile, however even in this case the localisation of strong velocity shear region is not perfect. A more reliable velocity profile can be obtained from the PCR data as a result of iteration procedure based on (4) and (5).

Conclusions

Simple explicit analytical expressions for the poloidal correlation reflectometry signal and cross correlation function accounting for probing wave diffraction in realistic 3D experimental geometry are given for arbitrary plasma density and turbulence profiles. It is shown that the reflectometry signal and turbulence spatial distributions can be very different. The simple method for the density perturbation reconstruction from the experimental data is proposed, however it is shown that for the concave density profile its accuracy decreases. The accuracy of simplified method of poloidal velocity determination from the PCR data can be as well affected by contribution of the plasma volume to the reflectometry signal for some density profiles and velocity distributions. The obtained explicit expressions for the PCR characteristics provide the effective theoretical tool for determination of the turbulence level and velocity distribution from the experimental data for arbitrary density profiles.

The work was supported by RFBR grant 04-02-16534; NWO-RFBR grants 047.016.015, Scientific School grant 2159.2003.2 and INTAS grants INTAS-01-2056.

References

1. V.A. Vershkov, S.V. Soldatov, D.A. Shelukhin et al. (2003) *Proc. 30th Conf. Control. Fusion Plasma Phys.* ECA 27A P-2.56

2. E.Z.Gusakov, A.V. Surkov (2004) *Plasma Phys. Control. Fusion* 46 1143–1162